Highly Efficient and Spectrally Stable Blue-Light-Emitting Polyfluorenes Containing a Dibenzothiophene-*S*,*S*-dioxide Unit

Jie Liu, Jianhua Zou, Wei Yang,* Hongbin Wu, Chun Li, Bin Zhang, Junbiao Peng, and Yong Cao*

Institute of Polymer Optoelectronic Materials and Devices, Key Laboratory of Specially Functional Materials, South China University of Technology, Guangzhou 510640, P.R. China

Received January 13, 2008. Revised Manuscript Received April 18, 2008

Spectrally stable blue-light-emitting polyfluorenes with high efficiency were realized via incorporating dibenzothiophene-*S*,*S*-dioxide (SO) isomer (3,7-diyl or 2,8-diyl) into the poly[9,9-bis(4-(2-ethylhexyloxy)phenyl)fluorene-2,7-diyl] (PPF) backbone. The resulting polymers have high fluorescence yield and exhibit very good thermal stability. The EL spectra of all copolymers remain almost unchanged, and no green emission is observed even at high applied current density (more than 360 mA/cm^2) or high annealing temperature(∼200 °C). With the device configuration ITO/PEDOT:PSS/PVK/emissive layer/Ba/Al, a maximum luminous efficiency (LE) of 6.0 cd/A (corresponding to an external quantum efficiency (EQE) of 5.5%) at 69 mA/cm^2 with CIE coordinates of (0.16, 0.19) for the polymer PPF-3,7SO20 and a maximum LE of 3.3 cd/A (EQE = 4.2%) with CIE coordinates of (0.16, 0.08) for the polymer PPF-2,8SO5 were obtained, respectively. The results indicate that this approach is very promising to obtain spectrally stable blue-light-emitting polyfluorenes with high efficiency.

Introduction

In recent years, there has been considerable interest in developing stable blue-light-emitting polymers with high efficiency. Despite plenty of effort from many groups, only a limited number of polymers exhibit promising performance as polymer light-emitting diodes (PLEDs).[1–3] Among them, polyfluorenes (PFs) have emerged as the most attractive blue emitters due to their high luminescent efficiency.[4] In addition, PFs can be easily functionalized at the 9-position of the fluorene unit with several alkyl groups. However, one of the most serious drawbacks of PFs is red-shifted emission after thermal annealing or upon long-term operation, which induces color impurity and is often associated with gradual material and device degradation.[5] One possible degradation mechanism in polyfluorene is formation of fluorenone defects upon thermal or photo-oxidation in the presence of oxygen.[6,7] Two strategies have often been employed to solve the problem, including copolymerization with suitable comonomer[8] and functionalization at the 9-position of fluorene. Li et al.[9] developed novel fluorene- and phenylene-based blue-light-emitting polymers. The improved spectral stability was attributed to the electron-withdrawing sulfonate group substituted on the phenylene backbone. Holmes et al.[10] synthesized defect-free 9,9-dioctyl-9*H*-fluorene via an alkylative cyclization route, which exhibited minimal green emission attributable to fluorenone formation. Huang et al.[11] introduced spiro-fluorene into the polyfluorene, backbone resulting in narrower emission with a smaller tail at longer wavelength. Müllen et al. introduced triphenylamine at the 9-position of fluorene[12a] and developed fully arylated poly(ladder-type-pentaphenylene),[12b] which suppressed the long-wavelength emission. Alkoxyphenyl substitution at the

* To whom correspondence should be addressed. E-mail: pswyang@scut.edu.cn; poycao@scut.edu.cn.

(1) (a) Ng, S.; Lu, H.; Chan, H. S. O.; Fujii, A.; Laga, T.; Yoshino, K. *Adv. Mater.* **2000**, *12*, 1122. (b) Woudenbergh, T. V.; Wildeman, J.; Blom, P. W. M.; Bastiaansen, J. J. A. M.; Langeveld-Voss, B. M. W. *Adv. Funct. Mater.* **2004**, *14*, 677. (c) Aharon, E.; Albo, A.; Kalina, M.; Frey, G. L. *Adv. Funct. Mater.* **2006**, *16*, 980. (d) Culligan, S. W.; Geng, Y.; Chen, S. H.; Klubek, K.; Vaeth, K. M.; Tang, C. W. *Adv. Mater.* **2003**, *15*, 1176.

(2) (a) Yan, H.; Huang, Q.; Cui, J.; Veinot, J. G. C.; Kern, M. M.; Marks, T. J. *Adv. Mater.* **2003**, *15*, 835. (b) Shih, H.; Lin, C.; Shih, H.; Cheng, C. *Adv. Mater.* **2002**, *14*, 1409. (c) Li, Y.; Fung, M. K.; Xie, Z.; Lee, S.; Huang, L.; Shi, J. *Adv. Mater.* **2002**, *14*, 1317. (d) Wu, C.; Lin, Y.; Wong, K.; Chen, R.; Chien, Y. *Adv. Mater.* **2004**, *16*, 61.

(3) (a) Suh, M. C.; Chin, B. D.; Kim, M.; Kang, T. M.; Lee, S. T. *Adv. Mater.* **2003**, *15*, 1254. (b) Lo, S.; Fichards, G. J.; Markham, J. P. J.; Namdas, E. B.; Sharma, S.; Burn, P. L.; Samuel, I. D. W. *Adv. Funct. Mater.* **2005**, *15*, 1451. (c) Chan, L.; Yeh, H.; Chen, C. *Adv. Mater.* **2001**, *13*, 1637. (d) Lu, H; Liu, C.; Chang, C.; Chen, S. *Adv. Mater.* **2007**, *19*, 2574.

(4) (a) Bernius, M. T.; Inbasekaran, M.; O'Brien, J.; Wu, W. S. *Adv. Mater.* **2000**, *12*, 1737. (b) Scherf, U.; List, E. J. W. *Adv. Mater.* **2002**, *14*, 477. (c) Babel, A.; Jenekhe, S. A. *Macromolecules.* **2003**, *36*, 7759.

(5) Bliznyuk, V. N.; Carter, S. A.; Scott, J. C.; Klärner, G.; Miller, R. D.; Miller, D. C. *Macromolecules* **1999**, *32*, 361.

(6) (a) List, E. J. W.; Guentner, R.; de Freitas, P. S.; Scherf, U. *Adv. Mater.* **2002**, *14*, 374. (b) Jacob, J.; Zhang, J. Y.; Grimsdale, A. C.; Müllen, K.; Gaal, M.; List, E. J. W. *Macromolecules* **2003**, *36*, 8240. (c) Gong, X.; Iyer, P. K.; Moses, D.; Bazan, G. C.; Heeger, A. J.; Xiao, S. S. *Adv. Funct. Mater.* **2003**, *13*, 325.

(7) (a) Nikitenko, V. R.; Lupton, J. M. *J. Appl. Phys.* **2003**, *93*, 5973. (b) Sims, M.; Bradley, D. D. C.; Ariu, M.; Koeberg, M.; Asimakis, A.; Grell, M.; Lidzey, D. G. *Adv. Funct. Mater.* **2004**, *14*, 765. (c) Becker, K.; Lupton, J. M.; Feldmann, J.; Nehls, B. S.; Galbrecht, F.; Gao, D. Q.; Scherf, U. *Adv. Funct. Mater.* **2006**, *16*, 364.

(8) Marsitzky, D.; Scott, J. C.; Chen, J.; Lee, V. Y.; Miller, R. D.; Setayesh, S.; Müllen, K. *Adv. Mater.* **2001**, *13*, 1096.

(9) Li, J.; Ziegler, A.; Wegner, G. *Chem. Eur. J.* **2005**, *11*, 4450.

(10) Cho, S. Y.; Grimsdale, A. B.; Jones, D. J.; Watkins, S. E.; Holmes, A. B. *J. Am. Chem. Soc.* **2007**, *129*, 11910.

(11) Yu, W; Pei, J.; Huang, W.; Heeger, A. J. *Adv. Mater.* **2000**, *12*, 828.

(12) (a) Ego, C.; Grimsdale, A. C.; Uckert, F.; Yu, G.; Srdanov, G.; Müllen, K. *Adv. Mater.* **2002**, *14*, 809. (b) Jacob, J.; Sax, S.; Gaal, M.; List, E. J. W.; Grimsdale, A. C.; Müllen, K. *Macromolecules* **2005**, *38*, 9933.

10.1021/cm800129h CCC: $40.75
Published on Web 06/11/2008

9-position of fluorene is an effective way to suppress the long-wavelength emission.[13,14] Lee et al.[15] prepared a homopoly[9,9-bis(4′-*n*-octyloxyphenyl)fluorene-2,7-diyl] (PBOPF). Although a stable blue emission with CIE coordinates of (0.136, 0.162) was obtained, the luminous efficiency of the device was as low as 0.03 cd/A. We found that introduction of *m*-dibenzothiophene into the polyfluorene backbone could effectively suppress the long-wavelength emission.[16] Furthermore, Miller et al.[17] reported the use of diphenylsolfone as an electron-transporting unit in polyfluorenes.

Recently, dibenzothiophene-*S*,*S*-dioxide was incorporated into the small molecules[18a,b] or polymers[18c] owing to its high fluorescence efficiency and electron affinity energy. Perepichka et al.[19] incorporated (3,7-diyl) dibenzothiophene-*S*,*S*-dioxide unit into the oligo-fluorenes and observed no green emission in the PL spectra after thermal annealing.

In this paper, we introduced dibenzothiophene-*S*,*S*-dioxide (SO) isomer (3,7-diyl or 2,8-diyl) into the poly[9,9-bis(4-(2-ethylhexyloxy)phenyl)fluorene-2,7-diyl] (PPF) backbone and investigated their electroluminescent properties based on the following considerations: first, the alkoxylphenyl groups substituted at the 9-position of the fluorene unit can suppress long-wavelength emission; second, the electron-withdrawing SO_2 group of SO unit would reduce the electron density of the PPF backbone, which is more resistant against the oxidation and formation of keto-detects; and, third, introduction of the SO unit can effectively improve electron injection and further enhance the electroluminescent properties.

Results and Discussion

Synthesis and Characterization of the Polymers. The chemical structures and synthetic route are shown in Scheme 1. The SO units were incorporated into the polyfluorene backbone through Suzuki polycondensation (SPC). The monomer feed molar ratios of PF/3,7SO as well as PF/2,8SO are 100:0, 95:5, 90:10, and 80:20 and 99:1, 97:3, 95:5, 93:7, and 90:10, and the corresponding polymers are referred to as PPF, PPF-3,7SO5, PPF-3,7SO10, and PPF-3,7SO20 and PPF-2,8SO1, PPF-2,8SO3, PPF-2,8SO5, PPF-2,8SO7, and PPF-2,8SO10, respectively. The actual molar ratios of the SO unit in the copolymers were calculated using elemental analysis and found to be very close to the feed molar ratios, as listed in Table 1. All polymers are soluble in common organic solvents, such as toluene, chloroform, THF, etc. The number-average molecular weight (M_n) of the polymers was determined by gel permeation chromatography (GPC) with THF as the eluent. For PPF-3,7SO and PPF-2,8SO copolymers, M_n ranges from 19 000 to 28 600 with polydispersity indices (PDI) ranging from 1.58 to 1.90 and from 14 300 to 35 600 with PDI ranging from 1.71 to 2.04, against polystyrene standards, respectively (Table 1).

Scheme 1. Synthetic Route of the Polymers [a]

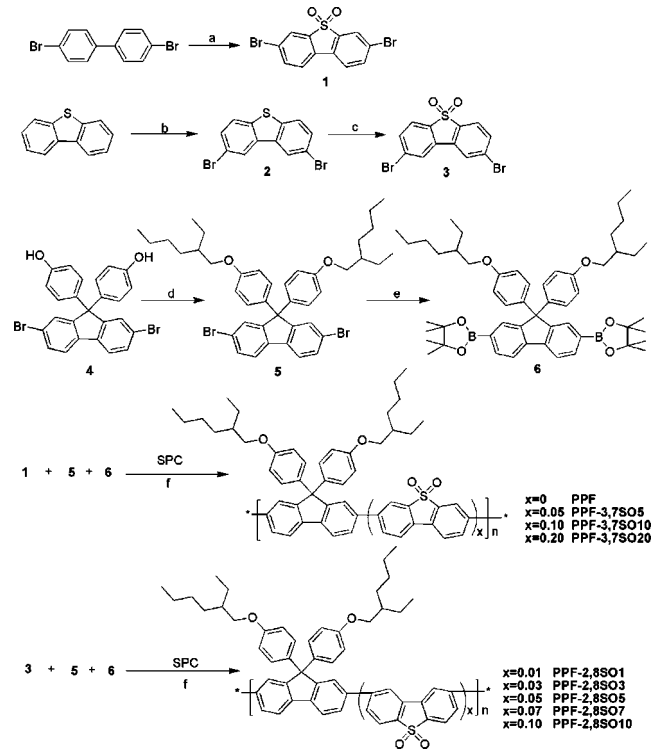

[a] Conditions: (a) CH_2Cl_2, HSO_3Cl, <50 °C; (b) $CHCl_3$, Br_2, Fe; (c) CH_3COOH, H_2O_2; (d) EtOH, KOH, EHBr; (e) THF, n-BuLi, −78 °C, 2-isopropoxy-4,4,5,5-tetramethyl-1,3,2-dioxaboralane; (f) $Pd(OAc)_2$, tricyclohexylphosphine, Et_4NOH, H_2O, toluene, THF.

Thermal Properties. The thermal properties of polymers were evaluated by thermogravimetric analyses (TGA) and differential scan calorimetry (DSC). The decomposition temperature (T_d, corresponding to 5 wt % loss) and glass-transition temperature (T_g) for homopolymer PPF are 408 and 148 °C, respectively, as shown in Table 1. We can see that the T_ds and T_gs of copolymers are much higher than that of PPF and increase with increasing content of the SO unit in the copolymers. The improved thermal stabilities were attributed to introduction of the polar and unsubstituted SO unit into the polyfluorene backbone.

Photophysical Properties. The absorption and PL spectra of PPF-3,7SO20 and PPF-2,8SO10 in different solvents are shown in Figure 1. The emissions of PPF-3,7SO20 have a stepwise red shift from toluene to DMF with increasing solvent polarity, while the absorption spectra are almost unchanged except in DMF solution (Figure 1). This indicates that the extent of intramolecular charge transfer (ICT) is greater in the excited state than in the ground state.[20] In contrast, the optical properties of PPF-2,8SO10 are affected

(13) Hwang, D. H.; Park, M. J.; Lee, J. H. *Mater. Sci. Eng.* **2004**, *C24*, 201.
(14) Lindgren, L. J.; Wang, X.; Inganäs, O.; Andersson, M. R. *Synth. Met.* **2005**, *154*, 97.
(15) Lee, J.; Hwang, D. *Chem. Commun.* **2003**, 2836.
(16) Yang, W.; Hou, Q.; Liu, C.; Niu, Y.; Huang, J.; Yang, R.; Cao, Y. *J. Mater. Chem.* **2003**, *13*, 1351.
(17) Miller, R. D.; Klaerner, G.; Fuhrer, T.; Kreyenschmidt, M.; Kwak, J.; Lee, V.; Chen, W.-D.; Scott, J. C *Nonlinear Optics, Principles, Materials, Phenomena, and Devices,* **1999**, *20* (1−4), 269.
(18) (a) Huang, T.; Lin, J. T.; Chen, L.; Lin, Y.; Wu, C. *Adv. Mater.* **2006**, *18*, 602. (b) Huang, T.; Whang, W.; Shen, J. Y.; Wen, Y.; Lin, J. T.; Ke, T.; Chen, L.; Wu, C. *Adv. Funct. Mater* **2006**, *16*, 1449. (c) Mikroyannidis, J. A.; Moshopoulou, H. A.; Anastasopoulos, J. A.; Styllanakis, M. M.; Fenenko, L.; Adachi, C. *J. Polym. Sci., Part A: Polym. Chem.* **2006**, *44*, 6790.
(19) Perepichka, I. I.; Perepichka, I. F.; Bryce, M. R.; Pålsson, L. *Chem. Commun.* **2005**, 3397.
(20) Zhu, Y.; Gibbons, K. M.; Kulkarni, A. P.; Jenekhe, S. A. *Macromolecules* **2007**, *40*, 804.

Table 1. Physical and Electrochemical Properties of the Polymers

polymer	M_n ($\times 10^3$)	PDI	SO unit (mol%) in feed ratio	SO unit (mol%) in polymer	T_d[a](°C)	T_g (°C)	HOMO/E_{ox} (eV/V)	LUMO (eV)[b]	E_g[c] (eV)	Φ_{PL}(%)
PPF	28.6	1.9	0		408	148	−5.87/1.47	−2.92	2.95	49
PPF-3,7SO5	20.3	1.8	5	4.97	428	167	−5.96/1.56	−3.04	2.92	56
PPF-3,7SO10	19.0	1.7	10	9.55	425	170	−5.96/1.56	−3.09	2.87	58
PPF-3,7SO20	23.6	1.6	20	18.31	431	192	−5.96/1.56	−3.11	2.85	59
PPF-2,8SO1	30.8	2.0	1	0.91	408	151	−5.92/1.52	−2.97	2.95	55
PPF-2,8SO3	35.6	1.9	3	3.79	412	158	−5.94/1.54	−3.00	2.94	55
PPF-2,8SO5	14.3	1.8	5	4.70	424	161	−5.96/1.56	−3.00	2.96	59
PPF-2,8SO7	16.0	1.9	7	6.75	424	173	−5.97/1.57	−3.01	2.96	59
PPF-2,8SO10	17.6	1.7	10	9.65	431	180	−5.98/1.58	−3.02	2.96	56

[a] Corresponding to 5 wt % loss. [b] Estimated from HOMO levels and the optical band gaps. [c] Calculated from the absorption spectra threshold.

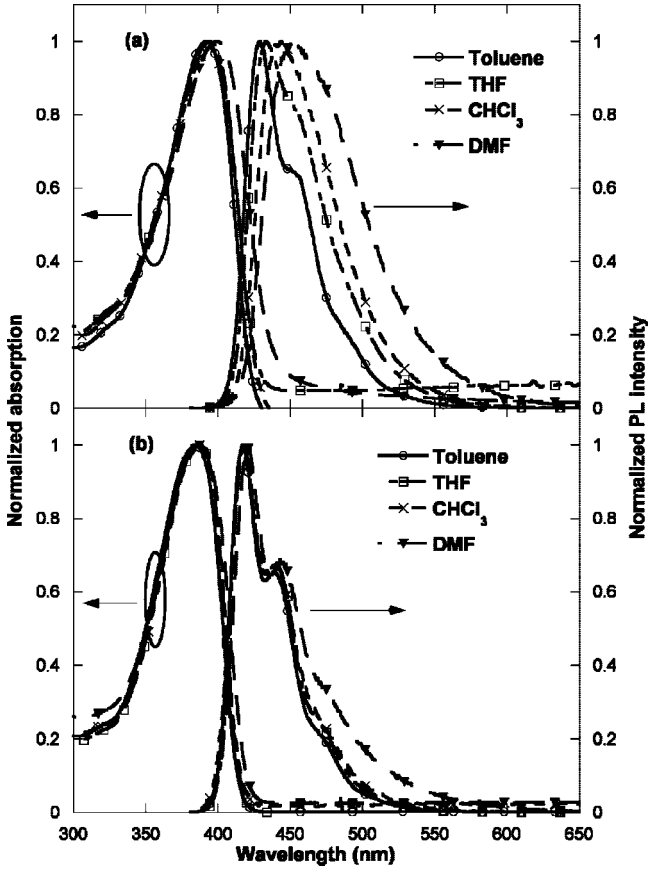

Figure 1. Absorption and PL spectra of 10^{-5} M solution for PPF-3,7SO20 (a) and PPF-2,8SO10 (b) in different solvents.

slightly by the solvent polarity (Figure 1b), indicating that introduction of the meta-linkage dibenzothiophene-*S*,*S*-dioxide unit into the polymer backbone can suppress the ICT interaction. Figure 2 displays the absorption spectra of the resulting polymers in the film. The polymers show only one distinct absorption band, which can be attributed to the $\pi-\pi^*$ transition of the conjugated polymer backbone.[18c] The optical band gaps E_gs of copolymers are derived from the onset of absorption spectra in the film. It is shown that the E_gs of PPF-3,7SOs copolymers become narrower and those of PPF-2,8SO copolymers are similar with homopolymer (Table 1). The absorption spectra reveal a general trend of steadily increased red shift with increasing content of 3,7SO unit compared to PPF (Figure 2a). The phenomenon of the red-shifted spectrum results from the intramolecular charge transition (ICT) existing between the donor fluorene and

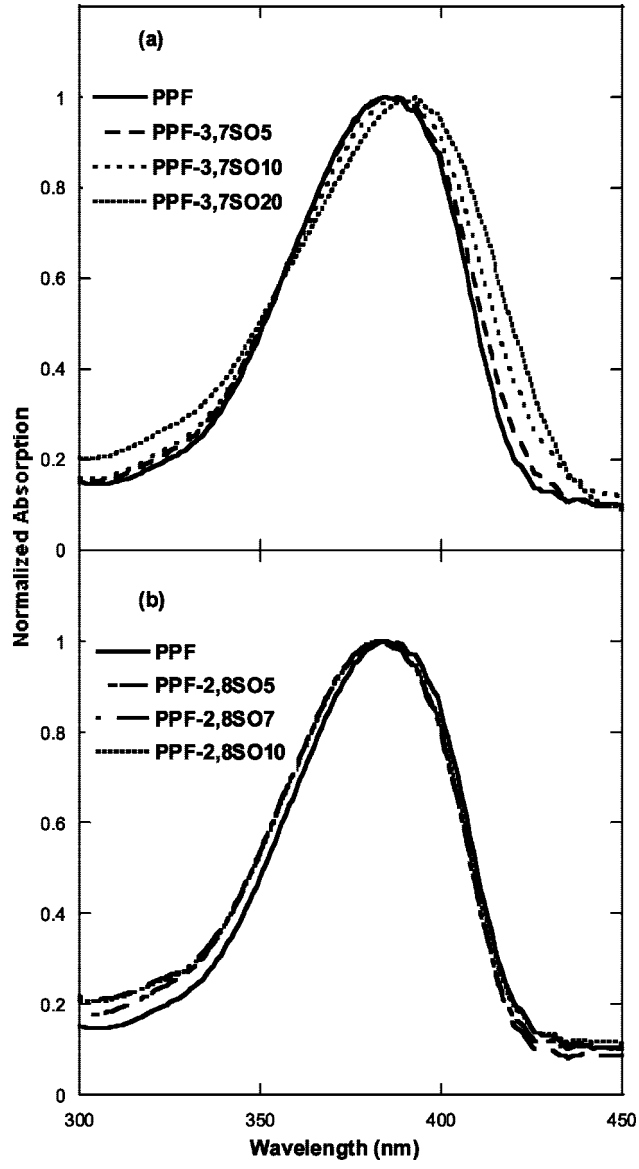

Figure 2. UV−vis absorption spectra of the polymers PPF-3,7SOs (a) and PPF-2,8SOs (b) in film.

acceptor SO moieties in the polymer backbone.[20] In contrast, the absorption spectra of PPF-2,8SOs are similar with that of PPF (Figure 2b). It is presumably attributed to introduction of the meta-linkage dibenzothiophene-*S*,*S*-dioxide unit into the polymer backbone, which can effectively disturb the effective conjugation length, which offsets the ICT effect.

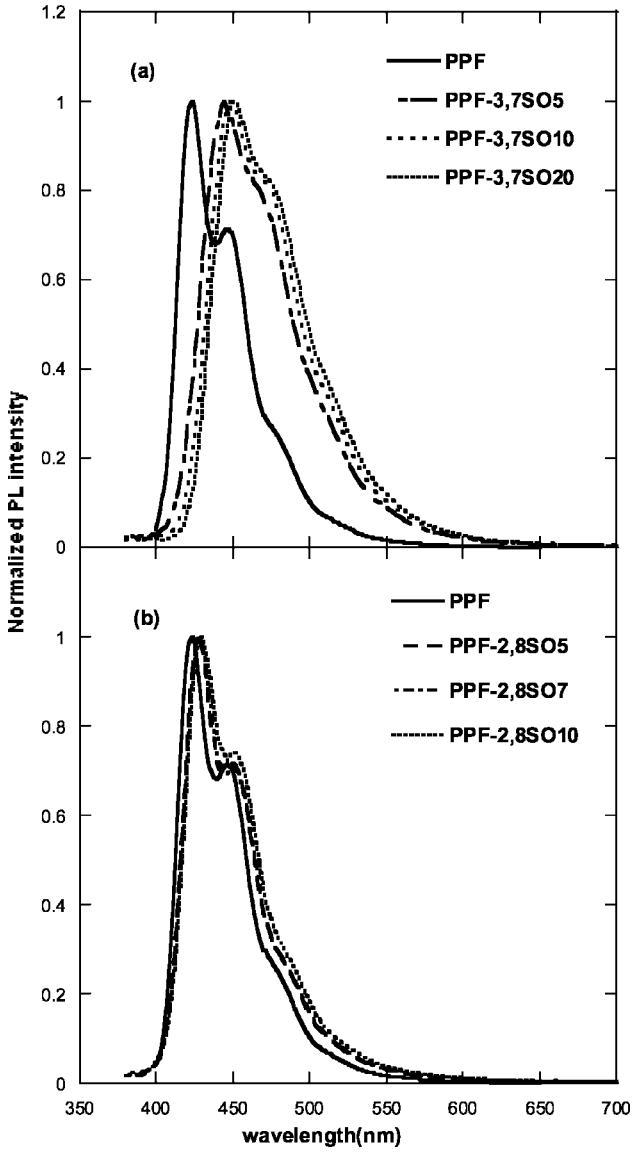

Figure 3. PL spectra of the polymers PPF-3,7SOs (a) and PPF-2,8SOs (b) in film.

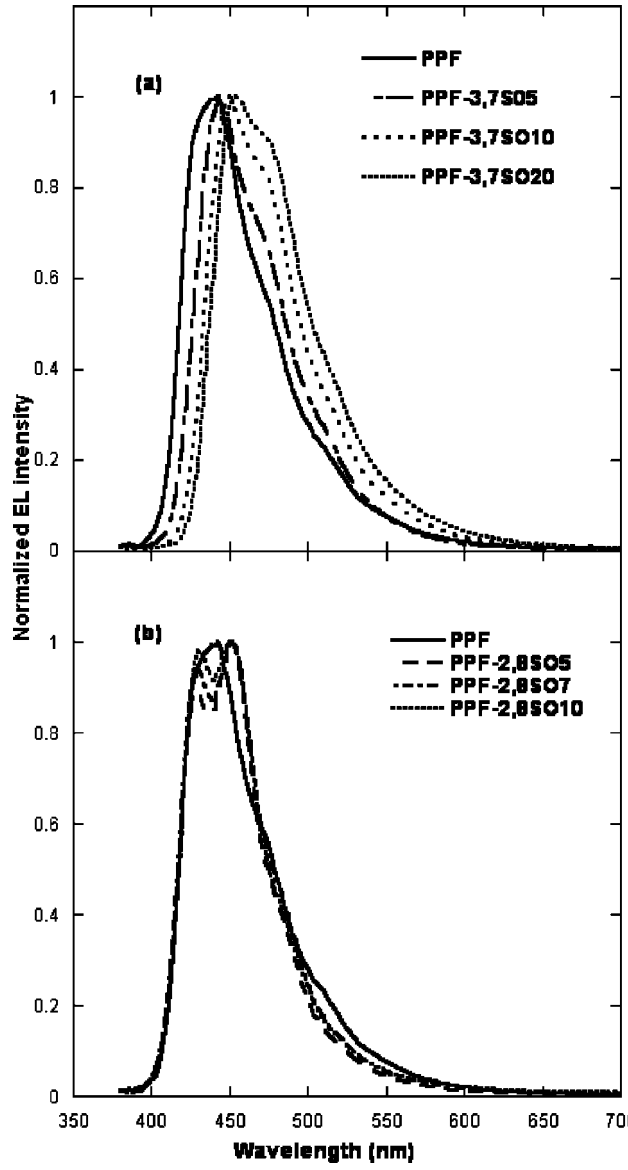

Figure 4. EL spectra of the polymers PPF-3,7SOs (a) and PPF-2,8SOs (b).

Photoluminescence (PL) spectra of the PPF-3,7SOs and PPF-2,8SOs in film are presented in Figure 3a and 3b, respectively. The PL spectra of PPF-3,7SOs are red shifted and broaden with increasing content of the 3,7SO unit, while those of PPF-2,8SOs are almost identical, which are consistent with those observed in the absorption spectra. It should be noted that the PL quantum efficiences (Φ_{PL}) of the copolymers are higher compared with PPF homopolymer (Table 1), the same as that of the dibenzothiophene-*S*,*S*-dioxide-fluorene co-oligomer.[19]

Electrochemical Properties. The electrochemical properties of the polymers were investigated by cyclic voltammetry (CV). The p-doping waves were recorded, but the n-doping process could not be detected in these copolymers (shown in Figure S1, Supporting Information). HOMO levels were calculated according to the empirical formula HOMO = $-e(E_{ox} + 4.4)$ (eV)[21] with the ferrocene oxidation potential as the standard for the vacuum energy level. LUMO levels were estimated from HOMO levels and the optical band gaps (E_g). As shown in Table 1, PPF has HOMO and LUMO levels at −5.87 and −2.92 eV, respectively. With increasing content of 3,7SO and 2,8SO units in the polymers, the LUMO levels of the copolymers decreased steadily compared to homopolymer PPF. This indicates that incorporation of an acceptor moiety into the polymer backbone lowers the LUMO level and, thus, could improve the electron-accepting ability of PPF.[22]

Electroluminescence. Devices with configuration ITO/poly(ethylendioxythiophene):poly(styrene sulfonic acid)(PEDOT:PSS)/poly(*N*-vinylcarbazole (PVK)/emissive layer/Ba/Al were fabricated. The EL spectra of devices based on PPF-3,7SOs and PPF-2,8SOs under 12 mA/cm^2 are shown in Figure 4a and 4b, respectively. The emission of PPF peaks at 440 nm, while for the copolymer PPF-3,7SOs the spectra are red shifted slightly with increasing content of 3,7SO unit.

(21) Bredas, J. L.; Silbey, R.; Boudreaux, D. S.; Chance, R. R. *J. Am. Chem. Soc.* **1983**, *105*, 6555.

(22) Wu, W.-C.; Liu, C.-L.; Chen, W.-C. *Polymer* **2006**, *47*, 527.

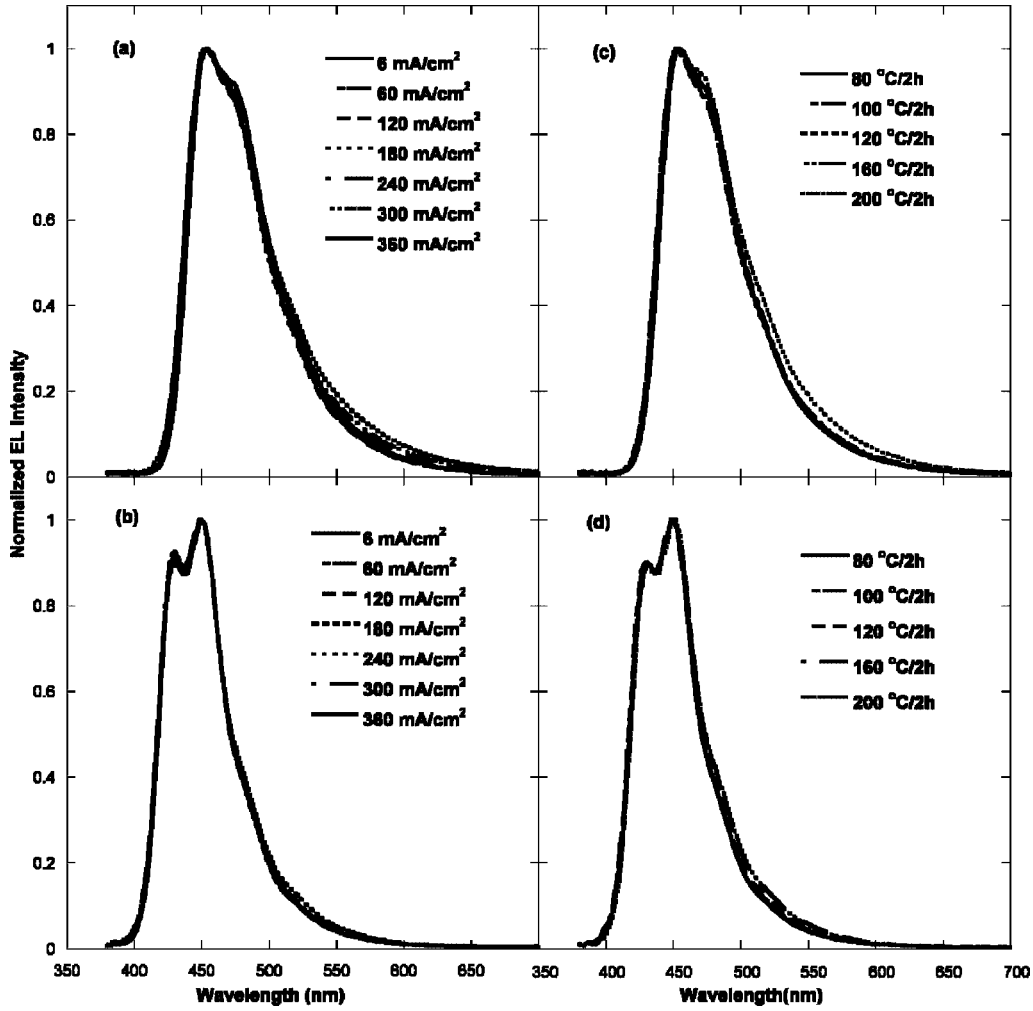

Figure 5. EL spectra of PPF-3,7SO20 and PPF-2,8SO5 under different applied current densities (a and b) and varied thermal annealing temperatures (c and d).

This is consistent with the trend for absorption of PPF-3,7SOs. In contrast, the EL spectra of PPF-2,8SOs show negligible deviation from that of the PPF.

In order to investigate the EL spectral stability, EL spectra dependences upon varied applied current densities and annealing temperatures were carried out. As shown in Figure 5a and 5b, taking PPF-3,7SO20 and PPF-2,8SO5 as examples, EL spectra of both copolymers are almost unchanged with the variation of applied current densities from 6 to 360 mA/cm^2. The same devices were annealed at 80, 120, 160, and 200 °C in turn for 2 h; the EL spectra remain very stable, and no green emission is observed, which often appears in fluorene-based polymers (Figure 5c and 5d). This is probably due to the combination of both bulk alkoxylphenyl substituted at the 9 position of the fluorene unit and the electron-withdrawing SO_2 group in the SO unit introduced into the polyfluorene backbone.

For the devices based on polymer PPF-3,7SOs, depending on the content of the SO unit, blue emission with CIE coordinates from (0.16, 0.13) to (0.16, 0.19) were realized. All of the devices exhibit high efficiencies, of which the device based on PPF-3,7SO20 exhibits the best overall performance in terms of the low turn on voltage of 5.4 V and a maximum luminous efficiency of 6.0 cd/A (corresponding to an EQE of 5.5%) at 69 mA/cm^2 with CIE coordinates of (0.16, 0.19). In parallel, the device performances for all of the copolymers are summarized in Table 2. As seen from Table 2, with increasing content of the 3,7SO unit the LE and EQE increase as well. On the other hand, the devices based on PPF-2,8SOs show an even bluer emission with CIE coordinates of (0.16, 0.08−0.09). For the device based on PPF-2,8SO5, a moderate turn on voltage of 5.0 V and maximum LE of 3.3 cd/A (EQE = 4.2%) with CIE coordinates of (0.16, 0.08) were realized. Figure 6 shows the typical luminous efficiency−luminance−current density (LE−L−J) characteristics of the devices based on PPF, PPF-2,8SO5, and PPF-3,7SO20,. It is clearly seen that the LE declines slightly with the increase of current density, indicating that the materials and devices have good stability. At a high current density of 100 mA/cm^2, LE of 4.0 cd/A (EQE = 3.8%) and LE of 2.3 cd/A (EQE = 2.9%) are still retained for the devices based on PPF-3,7SO20 and PPF-2,8SO5, corresponding to a luminance 4033 and 2291 cd/m^2, respectively. In addition, the efficiencies of all copolymers are superior to that of the homopolymer PPF (Table 2 and Figure 6). Figure 7 illustrates the relative energy levels of a device with the polymer PPF-3,7SO20. The HOMO and LUMO levels of the PPF-3,7SO20 are −5.96 and −3.11 eV, respectively. The hole injection barrier between PEDOT:PSS and PPF-3,7SO20 layers is 0.76 eV. Such a large barrier

Table 2. Device Performances of the Polymers

					J = 100 mA/cm^2				
polymer	V_{on} (V)[a]	L_{max} (cd/m^2)	LE_{max} (cd/A)	EQE_{max} (%)	V (V)	L (cd/m^2)	LE (cd/A)	EQE (%)	CIE[b]coordinates(x,y)
PPF	5.5	3615	2.2	2.1	9.6	1922	1.9	1.8	0.16, 0.12
PPF-3,7SO5	5.8	5585	3.3	3.0	11.9	2516	2.5	2.3	0.16, 0.13
PPF-3,7SO10	5.8	4921	3.5	3.2	10.9	3027	3.0	2.9	0.16, 0.16
PPF-3,7SO20	5.4	8339	6.0	5.5	9.1	4033	4.0	3.8	0.16, 0.19
PPF-2,8SO1	4.8	5104	2.4	3.0	9.1	1780	1.8	2.3	0.16, 0.08
PPF-2,8SO3	4.8	6126	2.6	3.3	9.4	1730	1.7	2.2	0.16, 0.08
PPF-2,8SO5	5.0	4767	3.3	4.2	9.8	2291	2.3	2.9	0.16, 0.08
PPF-2,8SO7	5.4	5587	2.4	3.0	10.2	1683	1.7	2.2	0.16, 0.09
PPF-2,8SO10	5.4	5030	2.7	3.5	10.3	866	0.9	1.2	0.16, 0.09

[a] Calculated with a luminance of 1 cd/m^2. [b] Measured at 12 mA/cm^2. Device structure: ITO/PEDOT:PSS/PVK/emissive layer/Ba/Al.

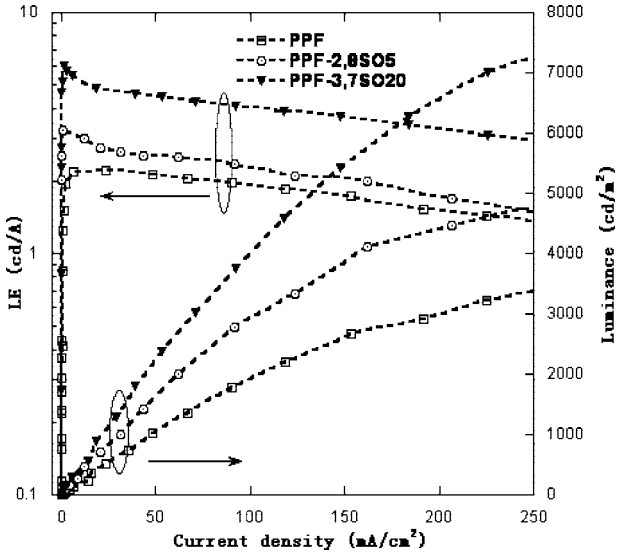

Figure 6. Luminous efficiency−luminance−current density curves of the devices based on polymers PPF, PPF-2,8SO5, and PPF-3,7SO20.

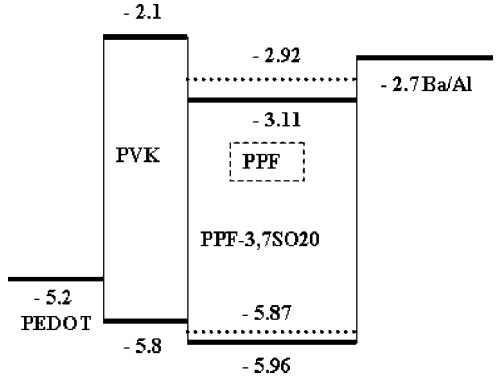

Figure 7. Energy-level diagram of the devices.

makes hole injection difficult, so inserting a PVK can serve as hole injection layer. On the other hand, the LUMO level of PPF-3,7SO20 decreased by 0.19 eV compared with PPF owing to the presence of the electron-withdrawing SO_2 group on the backbone. Electron injection from the cathode is easier for the copolymer than that for PPF. Therefore, the performances of the copolymers were improved.

It is worth pointing out that although the PPF-2,8SO series exhibits a higher maximum EQE than the PPF-3,7SO series, for example, 3.0% (PPF-3,7SO5) vs 4.2% (PPF-2,8SO5) and 3.2% (PPF-3,7SO10) vs 3.5% (PPF-2,8SO10), relatively lower LEs of PPF-2,8SOs than that of PPF-3,7SOs were observed. This can be understood since the emission of PPF-2,8SOs is located in the shorter wavelength region where the photo-optic response of the human eye is weaker than that of PPF-3,7SOs. High efficiency in combination with very stable deep-blue EL emission, which is very close to the CIE coordinates of National Television System Committee (NTSC) blue (0.14, 0.08), makes our polymer a good candidate as a blue emitter for display purposes.

Conclusion

Highly efficient and spectrally stable blue-light-emitting polyfluorenes were realized via incorporating dibenzothiophene-*S*,*S*-dioxide (SO) isomer (3,7-diyl or 2,8-diyl) into the poly[9,9-bis(4-(2-ethylhexyloxy)phenyl)fluorene-2,7-diyl] (PPF) backbone. EL spectra of all polymers remained almost unchanged, and no green emission was observed under different applied current densities as well as varied annealing temperatures due to the bulk alkoxyphenyl substituted at the 9-position of the fluorene unit and the electron-withdrawing SO_2 group in the SO unit introduced into the polyfluorene backbone. The efficiencies of all copolymers are superior to that of the homopolymer PPF, which could be attributed to the enhanced electron injection due to the SO unit in the polymer backbone and the balance between the electron and hole injection using PVK as a hole injection layer.

Experimental Section

Materials. Reagents were distilled from appropriate drying agents prior to use. Commercially available reagents were used without further purification. 2,7-Dibromo-9,9-bis-(4-hydroxyphenyl)fluorene (**4**),[14] 2,8-dibromodibenzothiophene (**2**),[16] and 2,8-dibromodibenzothiophene-*S*,*S*-dioxide (**3**)[23] were prepared according to the literature.

3,7-Dibromo-dibenzothiophene-*S*,*S*-dioxide (1). To a solution of 4,4-dibromodiphenyl (20 g, 64.1 mmol) in 50 mL of $CHCl_3$, was added sulfonic chloride acid (20 g, 172 mmol) slowly. During the addition the temperature was kept under 50 °C. Then the reaction mixture was stirred at room temperature for another 6 h. After the reaction was complete, the mixture was poured into ice−water and the excess acid was neutralized using $NaHCO_3$, the solid was filtered off and recrystallized from acetic acid to give needles, 5.6 g, yield 23.3%. ^{1}H NMR (300 MHz, $CDCl_3$) δ (ppm): 7.95 (d, J = 8.22 Hz, 2H), 7.79 (dd, J = 8.22, 1.77 Hz, 2H), 7.65 (d, J = 1.68 Hz, 2H). ^{13}C NMR: 138.96, 137.13, 129.60, 125.59, 124.60, 122.89. Anal. Calcd (%) for $C_{12}H_6SO_2Br$: C, 38.50; H, 1.60;

(23) Gilman, H.; Nobis, J. F. *J. Am. Chem. Soc.* **1945**, *67*, 1479.

S, 8.56; O, 8.56. Found: C, 38.49; H, 1.61; S, 8.41; O, 8.49. EIMS: *m*/*z* 375 $(M + 1)^+$.

2,7-Dibromo-9,9-bis(4-(2-ethylhexyloxy)phenyl)fluorene (5). **2** (11.5 g, 22.6 mmol) and KOH (5.06 g, 90.4 mmol) were mixed in 300 mL of EtOH. The reaction mixture was heated to 80 °C. After 0.5 h, 2-ethylhexane bromine (13.09 g, 67.8 mmol) was added into the reaction mixture dropwise. Then it was kept at 80 °C for 20 h. After the reaction was complete, the mixture was poured into 200 mL of water, extracted with ethyl acetic three times, and dried over $MgSO_4$. After removal of the organic solvent, a brown ropy liquid was obtained, purified by gel column chromatography using petroleum ether:ethyl acetic (95:5), and recrystallized from ethanol to afford white needles with a yield of 76% (12.5 g). ^{1}H NMR (300 MHz,$CDCl_3$) δ (ppm): 7.49 (d, $J = 2.34$ Hz, 2H), 7.46 (m, 4H), 7.07 (m, 4H), 6.78 (m, 4H), 3.81 (d, $J = 5.67$ Hz, 4H), 1.73 (m, 2H), 1.53−1.29 (br, 16H), 0.95−0.89 (m, 12H). ^{13}C NMR (75 MHz,CDCl3) δ (ppm): 162.58, 157.92, 141.97, 140.29, 134.82, 133.40, 133.08, 125.90, 125.62, 118.46, 74.45, 68.50, 43.49, 34.63, 33.19, 27.97, 27.15, 18.19, 15.23. Anal. Calcd (%) for $C_{41}H_{48}O_2Br$: C, 66.21; H, 6.56; O, 4.37. Found: C, 66.77; H, 6.37; O, 4.69. EIMS: *m*/*z* 733 $(M + 1)^+$.

2,7-Bis(4′,4′,5′,5′-tetramethyl-1′,3′,2′-dioxaboralan-2′-yl)-9,9-bis(4-(2-ethylhexyoxy)phenyl)fluorene (6). 2,7-Dibromo-9,9-bis(4-(2-ethylhexyloxy)phenyl)fluorene (6 g, 8.20 mmol) was added to 100 mL of dry THF and then cooled to −78 °C. *N*-Butyllithium was added dropwise to the solution, resulting a white viscous slurry. The mixture was stirred for 2 h at this temperature. Then 2-isopropoxy-4,4,5,5-tetramethyl-1,3,2-dioxaboralane was added in one portion. The reaction mixture was stirred for another 1 h at −78 °C and then up to room temperature for another 24 h. After the reaction was complete, the mixture was poured into 300 mL of ice−water and extracted with dichloromethane three times. The organic layer was combined and washed with water, brine, and water and dried over $MgSO_4$. After removal of the solvent the product was redissolved in THF and precipitated into methanol several times. A white product was obtained: 4.2 g, yield 62%. ^{1}H NMR (300 MHz,$CDCl_3$) δ (ppm): 7.79 (m, 6H), 7.13 (m, 4H), 6.74 (d, $J = 8.82$ Hz, 4H), 3.79 (d, $J = 5.64$ Hz, 4H), 1.68 (m, 2H), 1.28−1.54 (br, 40H), 0.95−0.88 (m, 12H). ^{13}C NMR: 157.99, 151.91, 142.65, 137.61, 134.07, 132.26, 129.42, 119.78, 114.00, 83.70, 70.27, 64.19, 39.43, 30.55, 29.11 24.93, 23.89, 23.08, 14.11, 11.15. Anal. Calcd (%) for $C_{53}H_{72}O_6B_2$: C, 76.99; H, 8.72; O, 11.62. Found: C, 77.11; H, 8.34; O, 11.96. EIMS: *m*/*z* 827 $(M + 1)^+$.

General Procedures for Suzuki Polycondensation Taking PPF-3,7SO20 as an Example. A mixture of monomer **1** (74.8 mg, 0.2 mmol), monomer **5** (217 mg, 0.297 mmol), monomer **6** (413 mg, 0.5 mmol), $Pd(acetate)_2$ (1.5 mg), and tricyclohexylphosphine (3 mg) was dissolved in a mixture of toluene (4 mL) and THF (4 mL) under an argon atmosphere. The mixture was heated to 90 °C and stirred; then $(Et)_4NOH$ (2 mL) and deionized water (2 mL) were added into the mixture. The solution was kept in the region of 90−100 °C with vigorous stirring under argon for 48 h. The end groups were capped by refluxing 6 h with monomer **3** and then bromobenzene, respectively. After cooling, the resulting polymer was precipitated into 100 mL of methanol, resolved in dichloromethane, and then washed three times with water. After removal of the solvent, the resulting polymers were received by precipitation in methanol. The resulted polymers were washed using acetone to remove oligomers and catalyst residues and dried under vacuo to give the anticipated polymers. Yield: 373 mg, 53%. ^{1}H NMR (300 MHz, $CDCl_3$) δ (ppm): 8.04−7.76 (br, 3.28H), 7.68−7.58 (br, 4H), 7.17 (br, 4H), 6.83 (m, 4H), 3.82 (d, 4H), 1.70 (s, 2H), 1.57−1.32 (br, 16H), 0.90 (m, 12H). Anal. Found (%) for PPF-3,7SO20: C, 76.33; H, 7.08; S, 1.16; O, 15.43.

PPF. Monomer **5** (364 mg, 0.497 mmol), monomer **6** (413 mg, 0.5 mmol), 484 mg, yield 62%. ^{1}H NMR (300 MHz, $CDCl_3$) δ (ppm): 7.77 (d, 2H), 7.55 (m,4H), 7.16 (m, 4H), 6.79 (d, 4H), 3.79 (d, 4H), 1.71−1.65 (br, 2H), 1.59−1.31 (br, 18H), 0.88−0.93 (m, 12H). ^{13}C (75 MHz, CDCl3) δ (ppm): 11.11, 14.09, 23.04, 23.84, 29.08, 30.52, 39.41, 64.35, 70.21, 114.14, 120.30, 124.70, 126.63, 129.18, 137.72, 138.78, 140.87, 152.84, 158.14. Anal. Found (%) for PPF: C, 84.80; H, 8.06; O, 7.14.

PPF-3,7SO5. Monomer **1** (18.7 mg, 0.05 mmol), monomer **5** (327 mg, 0.447 mmol), monomer **6** (413 mg, 0.5 mmol), 447 mg, yield 59%. ^{1}H NMR (300 MHz, $CDCl_3$) δ (ppm): 7.83−7.75 (br, 2H), 7.64−7.52 (br, 4H), 7.16 (br, 4H), 6.79 (br, 4H), 3.79 (d, 4H), 1.71−1.65 (br, 2H), 1.54−1.31 (br, 18H), 0.93−0.88 (m, 12H). Anal. Found (%) for PPF-3,7SO5: C, 85.77; H, 8.10; S, 0.29; O, 5.84.

PPF-3,7SO10. Monomer **1** (37.4 mg, 0.1 mmol), monomer **5** (290 mg, 0.397 mmol), monomer **6** (413 mg, 0.5 mmol), 403 mg, yield 54%. ^{1}H NMR (300 MHz, $CDCl_3$) δ (ppm): 8.03 (br, 0.26H), 7.83−7.76 (br, 2.24H), 7.65−7.52 (br, 4H), 7.17 (br, 4H), 6.79 (br, 4H), 3.80 (d, 4H), 1.68 (br, 2H), 1.56−1.32 (br, 18H), 0.90 (m, 12H). Anal. Found (%) for PPF-3,7SO10: C, 84.88; H, 7.86; S, 0.57; O, 6.69.

PPF-2,8SO1. Monomer **6** (413 mg, 0.5 mmol), monomer **5** (358 mg, 0.49 mmol), monomer **3** (3.7 mg, 0.01 mmol), white solid, 411 mg, yield 53%. ^{1}H NMR (300 MHz, $CDCl_3$) δ (ppm): 7.78 (br, 2H), 7.55 (m, 4H), 7.28−7.14 (br, 4H), 6.79 (d, 4H), 3.80 (d, 4H), 1.69 (br, 2H), 1.52−1.32 (br, 18H), 0.91 (m, 12H). Anal. Found (%) for PPFSO1: C, 86.52; H, 8.43; S, 0.24; O, 4.81.

PPF-2,8SO3. Monomer **6** (413 mg, 0.5 mmol), monomer **5** (344 mg, 0.47 mmol), monomer **3** (11.2 mg, 0.03 mmol), white solid, 399 mg, yield 52%. ^{1}H NMR (300 MHz, $CDCl_3$) δ (ppm): 7.88−7.78 (br, 2.10H), 7.55 (m, 4H), 7.28−7.14 (br, 4H), 6.79 (d, 4H), 3.80 (d, 4H), 1.69 (br, 2H), 1.52−1.32 (br, 18H), 0.91 (m, 12H). Anal. Found (%) for PPF-2,8SO3: C, 85.93; H, 8.39; S, 0.21; O, 5.47.

PPF-2,8SO5. Monomer **6** (413 mg, 0.5 mmol), monomer **5** (329 mg, 0.45 mmol), monomer **3** (18.7 mg, 0.05 mmol), white solid: 364 mg, yield 48%. ^{1}H NMR (300 MHz, $CDCl_3$) δ (ppm): 7.88−7.76 (br, 2.97H), 7.55 (m, 4H), 7.17 (br, 4H), 6.79 (d, 4H), 3.80 (d, 4H), 1.69 (br, 2H), 1.52−1.32 (br, 18H), 0.91 (m, 12H). Anal. Found[b] (%) for PPF-2,8SO5: C, 86.00; H, 8.35; S, 0.27; O, 5.38.

PPF-2,8SO7. Monomer **6** (413 mg, 0.5 mmol), monomer **5** (314 mg, 0.43 mmol), monomer **3** (26.2 mg, 0.07 mmol), white solid, 328 mg, yield 43%. ^{1}H NMR (300 MHz, $CDCl_3$) δ (ppm): 7.88−7.78 (br, 2.72H), 7.55 (m, 4H), 7.28−7.14 (br, 4H), 6.79 (d, 4H), 3.80 (d, 4H), 1.69 (br, 2H), 1.52−1.32 (br, 18H), 0.91 (m, 12H). Anal. Found [b](%) for PPF-2,8SO7: C, 86.12; H, 8.35; S, 0.39; O, 5.14.

PPF-2,8SO10. Monomer **6** (413 mg, 0.5 mmol), monomer **5** (292 mg, 0.40 mmol), monomer **3** (37.4 mg, 0.10 mmol), white solid, 296 mg, yield 48%. ^{1}H NMR (300 MHz, $CDCl_3$) δ (ppm): 7.88−7.78 (br, 2.98H), 7.55 (m, 4H), 7.28−7.14 (br, 4H), 6.79 (d, 4H), 3.80 (d, 4H), 1.69 (br, 2H), 1.52−1.32 (br, 18H), 0.91 (m, 12H). Anal. Found (%) for PPF-2,8SO10: C, 85.20; H, 8.25; S, 0.43; O, 6.12.

Measurements and Fabrication. ^{1}H and ^{13}C NMR spectra were recorded on a Bruker DRX 300 spectrometer operating, respectively, at 300 and 75 MHz in deuterated chloroform solution with tetramethylsilane as a reference. The MS of the compound were recorded on a LCQ DECA XP liquid chromatograph−mass spectrometer. The molecular weights of the polymers were determined by a Waters GPC 2410 in tetrahydrofuran (THF). Cyclic voltammetry (CV) data were measured on a CHI660A electro-

chemical workstation using Bu_4NPF_6 (0.1 M) in acetonitrile as electrolyte at a scan rate of 50 mV/s at room temperature under the protection of argon. A platinum electrode coated with a thin polymer film was used as the working electrode. A Pt wire was used as the counter electrode, and a calomel electrode was used as the reference electrode. Elemental analyses were performed on a Vario EL elemental analysis instrument (Elementar Co.). Thermogravimetric analyses (TGA) were performed on a Netzsch TG 209 at a heating rate of 20 °C/min. Differential scan calorimetry (DSC) measurements were perform on a Netzsch DSC 204 under N_2 flow at heating and cooling rates of 20 °C/min. UV−vis absorption spectra were recorded on a HP 8453 spectrophotometer. The PL quantum yields were measured using an Integrating Sphere IS080 (LabSphere) to collect the emitted light in all directions under excitation of a 325 nm HeCd laser (Melles Griot). The current density−voltage−luminance (J−V−L) characteristics were collected using a Keithley 236 source measurement unit and a calibrated silicon photodiode. The luminance was calibrated by a PR-705 SpectraScan Spectrophotometer (Photo Research) with simultaneous acquisition of the EL spectra and CIE coordinates, driven by a Keithley model 2400 Vage-current source. The device fabrication process was described previously in the literature.[24] Except spin coating of PEDOT buffer layer, all of the device fabrication processes and measurement steps were carried out in a glovebox filled with nitrogen.

Acknowledgment. We thank the Ministry of Science and Technology of China (Project No. 2002CB613402) and the National Natural Science Foundation of China (No. 20574021, U0634003, and 50433030) for financial support.

Supporting Information Available: Cyclic voltammograms of the polymers (PDF). This material is available free of charge via the Internet at http://pubs.acs.org.

CM800129H

(24) Luo, J.; Li, X.; Hou, Q.; Peng, J.; Yang, W.; Cao, Y. *Adv. Mater.* **2007**, *19*, 1113.